

Quantum Control of Ultra-cold Atoms: Uncovering a Novel Connection between Two Paradigms of Quantum Nonlinear Dynamics

Jiao Wang^{1,2}, Anders S. Mouritzen^{3,4}, and Jiangbin Gong^{3,5*}

¹*Temasek Laboratories, National University of Singapore, 117542, Singapore*

²*Beijing-Hong Kong-Singapore Joint Center for Nonlinear and Complex Systems (Singapore), National University of Singapore, 117542, Singapore*

³*Department of Physics and Center of Computational Science and Engineering, National University of Singapore, 117542, Singapore*

⁴*Department of Physics and Astronomy, University of Aarhus, DK-8000, Aarhus C, Denmark*

⁵*NUS Graduate School for Integrative Sciences and Engineering, Singapore 117597, Singapore*

(Dated: November 14, 2018)

* Corresponding author: phygj@nus.edu.sg

Abstract

Controlling the translational motion of cold atoms using optical lattice potentials is of both theoretical and experimental interest. By designing two on-resonance time sequences of kicking optical lattice potentials, a novel connection between two paradigms of nonlinear mapping systems, i.e., the kicked rotor model and the kicked Harper model, is established. In particular, it is shown that Hofstadter's butterfly quasi-energy spectrum in periodically driven quantum systems may soon be realized experimentally, with the effective Planck constant tunable by varying the time delay between two sequences of control fields. Extensions of this study are also discussed. The results are intended to open up a new generation of cold-atom experiments of quantum nonlinear dynamics.

Key Words: kicked rotor model, optical lattice, ultracold atoms, Hofstadter's butterfly spectrum, kicked Harper model

I. INTRODUCTION

One main objective of the field of quantum control [1, 2] is to use controlled laser-matter interaction to explore new aspects of quantum dynamics and enhance our understanding of quantum coherence phenomena. Along this direction quantum control ideas and techniques are expected to be very useful for quantum simulation studies, i.e., using controlled quantum systems to simulate important models. To that end ultracold atoms and molecules offer promising opportunities due to experimental advances in Bose-Einstein condensation, the great controllability of ultracold systems by laser fields, and the long decoherence time of ultracold systems.

Motivated by our interest in understanding quantum coherence effects and their control in classically chaotic systems [3], our work here focuses on possible cold-atom realizations of fundamental models of quantum nonlinear dynamics. One important paradigm of quantum chaos is the kicked rotor model (KRM) [4, 5] whose scaled Hamiltonian can be written as

$$H_{KRM} = \frac{p^2}{2} + K \cos(q) \sum_n \delta(t - nT), \quad (1)$$

where q ($\in [0, 2\pi)$) and p are conjugate coordinate and momentum variables, and T is the period of the kicking potential. For a general value of T , the spectrum of H_{KRM} is discrete and the quantum diffusion of the momentum distribution saturates as a consequence of quantum destructive interference despite the unlimited classical diffusion. This has been well understood in terms of a one-dimensional Anderson disorder model [6]. Interestingly, if the period of the kicking potential T is on resonance with the quantum recurrence time of the quantum free rotor dynamics, i.e., T is a rational multiple of the latter, then the associated spectrum will in general consist of continuous bands and ballistic quantum diffusion emerges. These features of the quantum KRM have played a significant role in advancing our understanding of quantum nonlinear dynamics. They have also motivated the experimental realization of the KRM using cold atoms subject to kicking optical lattice potentials [7]. Indeed, with the joint efforts of about ten laboratories worldwide working on the cold-atom realization of the KRM [8, 9, 10], many important dynamical features of the quantum KRM and its variants have been observed.

Another paradigm of quantum nonlinear dynamics is the kicked Harper model (KHM)

[11, 12, 13, 14, 15]. Using similar notation as the KRM, the KHM Hamiltonian is given by

$$H_{KHM} = (L/T) \cos(p) + K \cos(q) \sum_n \delta(t - nT), \quad (2)$$

where L and K are two system parameters. For later use we note that the classical KHM map is given by

$$\begin{aligned} p_c(n+1) &= p_c(n) + K \sin[q_c(n)], \\ q_c(n+1) &= q_c(n) - L \sin[p_c(n+1)], \end{aligned} \quad (3)$$

where $[q_c(n), p_c(n)]$ denote the values of the classical coordinate and momentum right before $t = nT$. The quantum map associated with each period T is given by

$$U_{KHM} = e^{-i\frac{L \cos(p)}{\hbar}} e^{-i\frac{K \cos(q)}{\hbar}}, \quad (4)$$

where \hbar is the effective Planck constant in our scaled unit system (hence $p = -i\hbar\partial/\partial q$). For the critical case of $K = L$, the (quasi-energy) spectrum of the quantum map U_{KHM} is very similar to the famous Harper model for studies of two-dimensional electron gases in a strong magnetic field [16]. In particular, the spectrum of U_{KHM} with $K = L$ is a fractal, often called the ‘‘Hofstadter’s butterfly’’ spectrum [16]. As such, the dynamical properties of the KHM are often in sharp contrast to those in the KRM. Indeed, complementing the KRM, the KHM has been regarded as another important paradigm of quantum chaos, offering a test bed for understanding how a fractal spectrum is manifested in quantum mapping systems and how the underlying classical chaos affects the butterfly spectrum. One important question thus arises before the research community: How to experimentally realize or experimentally simulate the KHM?

Two previous studies have proposed to use Fermi-surface electrons in pulsed fields [23] or a charged particle kicked by a designed field sequence [24] to realize the KHM. However, these proposals, unrelated to ongoing cold-atom experiments of quantum chaos, have not led to experiments. An intriguing connection between the KHM and the so-called kicked harmonic oscillator model [25] might also help realize the KHM, but unfortunately this connection is subject to the strong restriction of $K = L$. By contrast, in a recent work [17], we have briefly reported that based on existing cold-atom experiments of the KRM, it should be possible to experimentally realize a quantum version of the KHM by making use of two sequences of kicking optical lattice potentials (i.e., making use of a double kicked

rotor system, to be explained later). This unveils for the first time a direct connection between the two paradigms of quantum nonlinear dynamics, i.e., the KRM and the KHM. In this paper, we present further discussions and important details of our finding. We shall emphasize that the effective Planck constant of our realization of the quantum KHM can be tuned by varying the time delay between two sequences of control fields, thus offering opportunities for understanding the differences and similarities between the quantum and classical dynamics. Extensions of our study to a wider class of periodically driven quantum systems are also discussed. It is our hope that this contribution can motivate more interest in quantum control and quantum simulation of classically chaotic systems.

II. KICKED HARPER MODEL REALIZED BY ON-RESONANCE DOUBLE-KICKED ROTOR MODEL

Our starting point is a modification of the standard KRM, called a double kicked rotor model (DKRM). That is, within each period T , the free evolution of a rotor is interrupted twice by external kicking potentials. Such a model has been experimentally realized [18] and has already attracted considerable interests [19, 20]. In terms of the scaled variables used above, the DKRM Hamiltonian is given by

$$H = \frac{p^2}{2} + K_1 \cos(q) \sum_n \delta(t - nT) + K_2 \cos(q) \sum_n \delta(t - nT - \eta). \quad (5)$$

Clearly, within each period T the rotor experiences two kicks at $t = nT$ and $t = nT + \eta$, with the two field amplitudes characterized by K_1 and K_2 . Hence, there are now two sequences of kicking fields with the same period T , and the time delay between the two sequences of control fields is given by η . The associated quantum map U_{DKRM} for a period from $nT + 0^-$ to $(n + 1)T + 0^-$ is found to be

$$U_{DKRM} = e^{-i(T-\eta)\frac{p^2}{2\hbar}} e^{-i\frac{K_2}{\hbar} \cos(q)} e^{-i\eta\frac{p^2}{2\hbar}} e^{-i\frac{K_1}{\hbar} \cos(q)}. \quad (6)$$

Note that for a Hilbert space satisfying the periodic boundary condition associated with $q \rightarrow q + 2\pi$, which should be the case for a rotor, the momentum eigenvalues can only take integer values multiplied by \hbar . Consider now what happens under the quantum resonance condition, i.e., $T\hbar = 4\pi$. Due to the discreteness of the momentum eigenvalues, one immediately

obtains $e^{-iT\frac{p^2}{2\hbar}} = 1$. Under this resonance condition, U_{DKRM} is reduced to U_{DKRM}^r ,

$$\begin{aligned} U_{DKRM}^r &= e^{i\eta\frac{p^2}{2\hbar}} e^{-i\frac{K_2}{\hbar} \cos(q)} e^{-i\eta\frac{p^2}{2\hbar}} e^{-i\frac{K_1}{\hbar} \cos(q)} \\ &= e^{i\frac{\tilde{p}^2}{2\tilde{\hbar}}} e^{-i\frac{\tilde{K}_2}{\tilde{\hbar}} \cos(q)} e^{-i\frac{\tilde{K}_1}{\tilde{\hbar}} \cos(q)}, \end{aligned} \quad (7)$$

where we have defined the rescaled momentum $\tilde{p} \equiv \eta p$ and the rescaled kicking amplitudes $\tilde{K}_1 \equiv \eta K_1$, $\tilde{K}_2 \equiv \eta K_2$. In terms of this rescaled momentum operator \tilde{p} , the effective Planck constant evidently becomes $\tilde{\hbar} \equiv \eta\hbar$. Certainly, in a cold-atom realization of this system, one should not forget that the cold atoms are actually moving in a flat space rather than in a compact angular space. Hence, the quantum resonance condition is relevant only when the initial quantum state is prepared in a state closely resembling a momentum eigenstate. This is already well within reach of today's experiments. For example, two recent experiments [9, 10] realized a KRM on quantum resonance, using a delocalized Bose-Einstein condensate that generates appropriate initial states.

Using the rescaled variables defined above and the associated effective Planck constant $\tilde{\hbar}$, the quantum map in Eq. (7) can now be interpreted in a straightforward manner. Specifically, within each period T , the system is first subject to one kick, followed by a free evolution interval; then the system is kicked a second time, followed by a second interval of free evolution, with the free Hamiltonian for the second free evolution interval given by $H_{\text{free}} = -\tilde{p}^2/2$. This interpretation makes it clear that the on-resonance double kicked rotor model realizes a modified kicked rotor we proposed in Ref. [21]. Equation (7) also indicates that the time delay η between the two sequences of the kicking fields offers a convenient means to vary $\tilde{\hbar} = \eta\hbar$. Hence, the effective Planck constant $\tilde{\hbar}$ of the quantum map obtained above can be easily tuned, so long as we keep \tilde{K}_1 and \tilde{K}_2 constant. This offers a promising opportunity for studies of the quantum-classical correspondence associated with the map U_{DKRM}^r .

Consider now a well-defined classical limit of the map U_{DKRM}^r , i.e. the $\eta \rightarrow 0$ limit or equivalently the $\tilde{\hbar} \rightarrow 0$ limit. Note that this special classical limit is based on the above on-resonance DKRM, and is hence unrelated to the conventional classical version of a DKRM (the conventional classical version of a DKRM is reached by letting $\hbar \rightarrow 0$ with fixed K_1 , K_2 , T , and η). Based on the above simple interpretation of U_{DKRM}^r , let us now consider the classical analogs of the quantum observables \tilde{p} and q right before $t = nT$. These classical quantities will be denoted $\tilde{p}_c(n)$ and $q_c(n)$, representing the values of classical canonical

variables right before $t = nT$. Then, after the combined action of the first kick at $t = nT$ and the first free evolution interval, $\tilde{p}_c(n)$ and $q_c(n)$ evolve to $\tilde{p}'_c(n)$ and $q'_c(n)$, with

$$\begin{aligned}\tilde{p}'_c(n) &= \tilde{p}_c(n) + \tilde{K}_1 \sin[q_c(n)], \\ q'_c(n) &= q_c(n) + \tilde{p}'_c(n).\end{aligned}\tag{8}$$

Similarly, after the combined action of the second kick and the second free evolution interval, the total elapsed time is T and $\tilde{p}'_c(n)$ and $q'_c(n)$ evolve to $\tilde{p}_c(n+1)$ and $q_c(n+1)$,

$$\begin{aligned}\tilde{p}_c(n+1) &= \tilde{p}'_c(n) + \tilde{K}_2 \sin(q'_c), \\ q_c(n+1) &= q'_c(n) - \tilde{p}_c(n+1).\end{aligned}\tag{9}$$

The overall classical map in the limit of $\tilde{\hbar} \rightarrow 0$, for the period between $nT + 0^-$ and $(n+1)T + 0^-$, can be found by considering the above two steps together, i.e.,

$$\begin{aligned}\tilde{p}_c(n+1) &= \tilde{p}_c(n) + \tilde{K}_2 \sin \left[q_c(n) + \tilde{p}_c(n) + \tilde{K}_1 \sin[q_c(n)] \right] + \tilde{K}_1 \sin[q_c(n)], \\ q_c(n+1) &= q_c(n) - \tilde{K}_2 \sin \left[q_c(n) + \tilde{p}_c(n) + \tilde{K}_1 \sin[q_c(n)] \right].\end{aligned}\tag{10}$$

At first glance this map seems rather complicated, but if we make a classical canonical transformation

$$(q_c, \tilde{p}_c) \rightarrow (Q_c = q_c, \tilde{P}_c = \tilde{p}_c + q_c),\tag{11}$$

then the map of Eq. (10) assumes a much simpler form,

$$\begin{aligned}\tilde{P}_c(n+1) &= \tilde{P}_c(n) + \tilde{K}_1 \sin[Q_c(n)], \\ Q_c(n+1) &= Q_c(n) - \tilde{K}_2 \sin[\tilde{P}_c(n+1)].\end{aligned}\tag{12}$$

Remarkably, with the substitutions $\tilde{K}_1 \rightarrow K$ and $\tilde{K}_2 \rightarrow L$, the map we obtained in Eq. (12) is identical with the classical KHM map in Eq. (3)! That is, for a DKRM under the resonance condition $T\tilde{\hbar} = 4\pi$, the quantum map U_{DKRM}^r is simply a quantum version of the KHM, insofar as its $\tilde{\hbar} \rightarrow 0$ classical limit is equivalent to a classical kicked Harper model. This surprising finding exposes a direct connection between the KHM and a kicked rotor system for the first time. Because the DKRM was experimentally realized a few years ago, the finding here indicates that our quantum version of the KHM can be realized by slightly modifying the previous experiments [18]. Considering the many fascinating dynamical features of the KHM, we hope that our work will be able to motivate many new cold-atom experiments of quantum nonlinear dynamics.

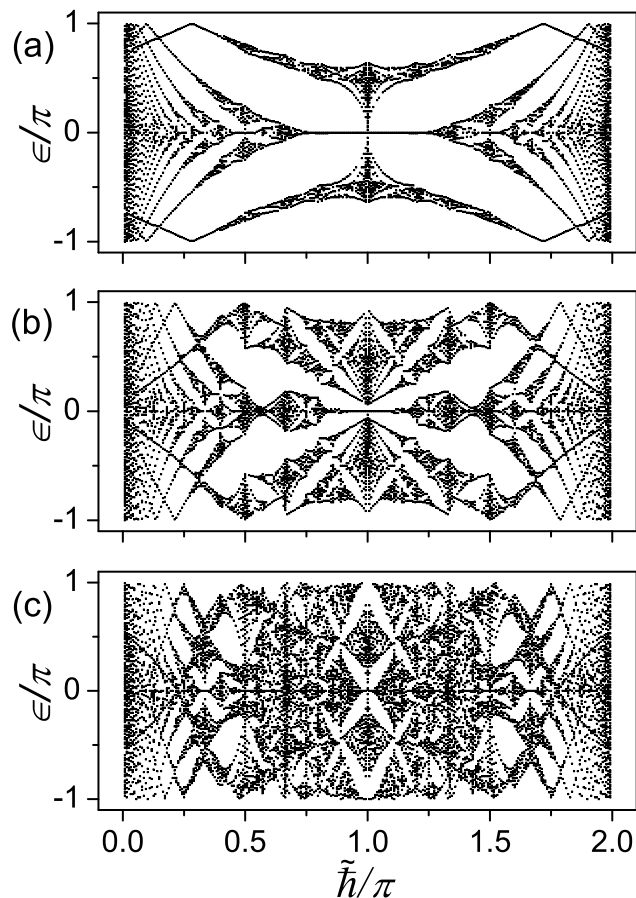


FIG. 1: Quasi-energy spectrum of the cold-atom realization of a quantum version of the kicked Harper model, achieved by considering a double kicked rotor model under the main quantum resonance condition $T\hbar = 4\pi$. For panels (a), (b), and (c), $\tilde{K}_1/\tilde{\hbar} = \tilde{K}_2/\tilde{\hbar} = 2.0, 3.0,$ and $4.0,$ respectively. The Hofstadter's butterfly spectrum seen here is almost indistinguishable from that calculated from the standard kicked Harper model.

III. DETAILED RESULTS

A. Hofstadter's butterfly spectrum

In Fig. 1 we show the quasi-energy spectrum of U_{DKRM}^r as a function of the effective Planck constant $\tilde{\hbar}$, for three values of $\tilde{K}_1/\tilde{\hbar} = \tilde{K}_2/\tilde{\hbar}$. The famous Hofstadter's butterfly structure can be clearly seen. Indeed, we have compared the spectrum of U_{DKRM}^r with that of the U_{KHM} in Eq. (4), for $\tilde{K}_1 = K = \tilde{K}_2 = L$ and for the same value of the effective Planck

constant. The result is that no difference in the Hofstadter's butterflies can be seen by the naked eye. For other parameters ($\tilde{K}_1 = K \neq \tilde{K}_2 = L$), the remarkable similarity is also observed (not shown). The fractal property of the spectrum of U_{DKRM}^r has also been checked carefully. For example, for $\tilde{K}_1 = \tilde{K}_2 = 1$, $\tilde{\hbar} = 2\pi/(1 + \sigma)$, and $\sigma = (\sqrt{5} + 1)/2$, the generalized fractal dimension [17] of the spectrum is found to be $D_0 \approx 0.5$. This is identical to that of the KHM, with $K = L = 1$ and the same value of the effective Planck constant.

The results in Fig. 1 bring up an interesting question. Is the butterfly spectrum of U_{DKRM}^r mathematically the same as that of the KHM? That is, does there always exist a unitary transformation to transform U_{KHM} in Eq. (4) to U_{DKRM}^r ? The answer is no. Even though a canonical transformation of the classical limit of U_{DKRM}^r is equivalent to the classical limit of U_{KHM} , their quantum spectra can still be different due to the periodic boundary condition associated with their Hilbert spaces. Qualitatively, this is because a classical canonical transformation does not necessarily have a unitary transformation analog in the quantum case. In other words, a particular quantization strategy can induce differences between the butterfly spectra of U_{DKRM}^r and that of U_{KHM} .

Especially, we have shown that for fixed K/\hbar and L/\hbar , the spectrum of U_{KHM} has a period 2π in \hbar , and is reflection symmetric about $\hbar = \pi$. By contrast, the spectrum of U_{DKRM}^r (for fixed $\tilde{K}_1/\tilde{\hbar}$ and $\tilde{K}_2/\tilde{\hbar}$) has a period 4π in $\tilde{\hbar}$, and is reflection symmetric about $\tilde{\hbar} = 2\pi$ instead. Also significant, it can be proved that the spectrum of U_{DKRM}^r is invariant if we swap \tilde{K}_1 and \tilde{K}_2 .

As an example of spectral differences, we find that so long as $\tilde{K}_1 \neq \tilde{K}_2$, the spectrum of U_{DKRM}^r is in general continuous. This is markedly different from the KHM, where the spectrum can change from being continuous to being discrete if we swap the values of K and L [13, 14]. Other subtle spectral differences between U_{DKRM}^r and U_{KHM} , especially those regarding the butterfly spectrum's sub-band widths in cases of $\tilde{\hbar} = \hbar = 2\pi r/s$ (r and s being integers), have also been studied [27] but will not be discussed here.

B. Quantum Diffusion Dynamics

Our cold-atom proposal for realizing one quantum version of the KHM has presented exciting opportunities for experimental studies of quantum diffusion dynamics with a butterfly spectrum. Though the fractal butterfly spectrum seen above is not a direct experimental

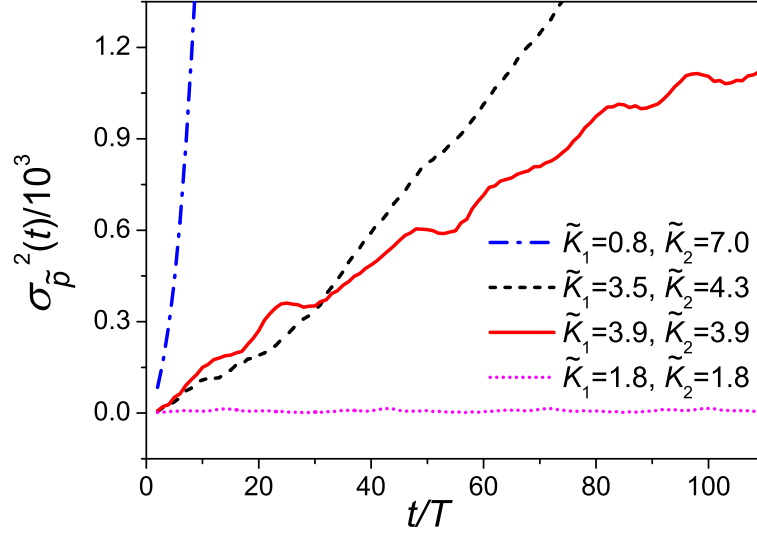


FIG. 2: Time dependence of the momentum variance $\sigma_{\tilde{p}}^2(t)$ in the cold-atom realization of the kicked Harper model. The main features range from localization, subdiffusion to almost ballistic diffusion. In the dotted line case $\tilde{\hbar} = 6\pi/19$; for other three cases $\tilde{\hbar} = 1$. The initial state is taken as a zero momentum state, which can be approximately realized by use of a dilute Bose-Einstein condensate with very large coherence length.

observable, the fractal properties of the spectrum do govern the quantum dynamics [26]. A number of previous studies have contributed to understanding the manifestations of a fractal spectrum in the quantum dynamics.

To motivate experimental work based on our finding we present here some remarkable numerical results of the quantum diffusion dynamics associated with U_{DKRM}^r . We choose to examine the time dependence of the momentum variance of a time-evolving wavepacket $|\varphi(t)\rangle$. This variance is given by $\sigma_{\tilde{p}}^2(t) \equiv \tilde{\hbar}^2 \sum_l |\langle \varphi(t)|l\rangle|^2 (l - l_0)^2$, where $\{|l\rangle\}$ are the eigenstates of \tilde{p} with the eigenvalue $l\tilde{\hbar}$, $|l_0\rangle$ is the initial state, and l_0 is the time-independent mean value of $\tilde{p}/\tilde{\hbar}$. Note that $\sigma_{\tilde{p}}^2(t)$ is a quantity easily measurable in current cold-atom experiments of the KRM. In our numerical calculations we assume $l_0 = 0$ but we have checked that the results presented below do not depend on the initial condition we choose.

First of all, for both $\tilde{K}_1 \ll \tilde{K}_2$ and $\tilde{K}_1 \gg \tilde{K}_2$, the dynamics of U_{DKRM}^r typically displays almost ballistic diffusion with $\sigma_{\tilde{p}}^2(t) \sim t^2$. One such example is represented by the dot-dashed line in Fig. 2. It is also computationally found that if we swap \tilde{K}_1 and \tilde{K}_2 , then the time

dependence of $\sigma_p^2(t)$ does not change. This feature is consistent with our previous discussion and does not exist in the dynamics of U_{KHM} .

Besides, for $\tilde{K}_1 = \tilde{K}_2$ and for a generic value of $\tilde{\hbar}$, the quantum diffusion dynamics is expected to be drastically different because the spectrum is a fractal (see Fig. 1). In Fig. 2 we show one such computational example with $\tilde{K}_1 = \tilde{K}_2 = 3.9$ and $\tilde{\hbar} = 1$ (solid line). It is seen that the quantum diffusion dynamics in this case is much slower than the previous ballistic diffusion case. To further understand this case we follow the dynamics over a time scale of $t = 10^4 T$ and then fit $\sigma_p^2(t)$ by a power law. This fitting yields $\sigma_p^2(t) \sim t^\alpha$ with the quantum diffusion exponent $\alpha \approx 0.82$, indicating an anomalous diffusion. Applying an existing theory [22] that relates the quantum diffusion exponent α to the fractal dimension of the spectrum, we infer that in the case of $\alpha \approx 0.82$, the Hausdorff-dimension of the fractal spectrum is $D_H \approx 0.41$. Interestingly, if we slightly mismatch \tilde{K}_1 and \tilde{K}_2 (dashed line in Fig. 2), then it is found that after a transient time of about $10^2 T$, $\sigma_p^2(t)$ will display ballistic diffusion like in the first example. As such, by merely slightly tuning the relative strengths of the two sequences of the control fields without even changing their average strength $(\tilde{K}_1 + \tilde{K}_2)/2$, one may generate many remarkable and qualitatively different features in the quantum diffusion dynamics.

Let us finally discuss the result of the dotted line in Fig. 2. In this case, $\tilde{\hbar} = 6\pi/19$, $\tilde{K}_1 = \tilde{K}_2 = 1.8$, and $\sigma_p^2(t)$ is seen to saturate at very small values. Computationally, this saturation behavior is found to persist for times larger than $10^6 T$. Hence the quantum diffusion dynamics in this case constitutes an example of strong localization. This localization behavior is related to the fact that the spectrum sub-band width of the butterfly of U_{DKRM}^r may become vanishingly small as $\tilde{K}_1 = \tilde{K}_2$ decreases [27]. We believe that the localization observed here represents a novel type of dynamical localization in quantum nonlinear dynamics. Our ongoing theoretical work will soon offer more insights into this [27]. Experimentally speaking, observing such kind of localization behavior would be a strong indication that our cold-atom version of the KHM has been cleanly realized.

C. Extension to Double Kicked Rotor Systems on Higher-Order Resonances

So far, we have shown that by considering a double kicked rotor under the resonance condition $T\hbar = 4\pi$, a cold-atom realization of the KHM is within reach of today's experiments.

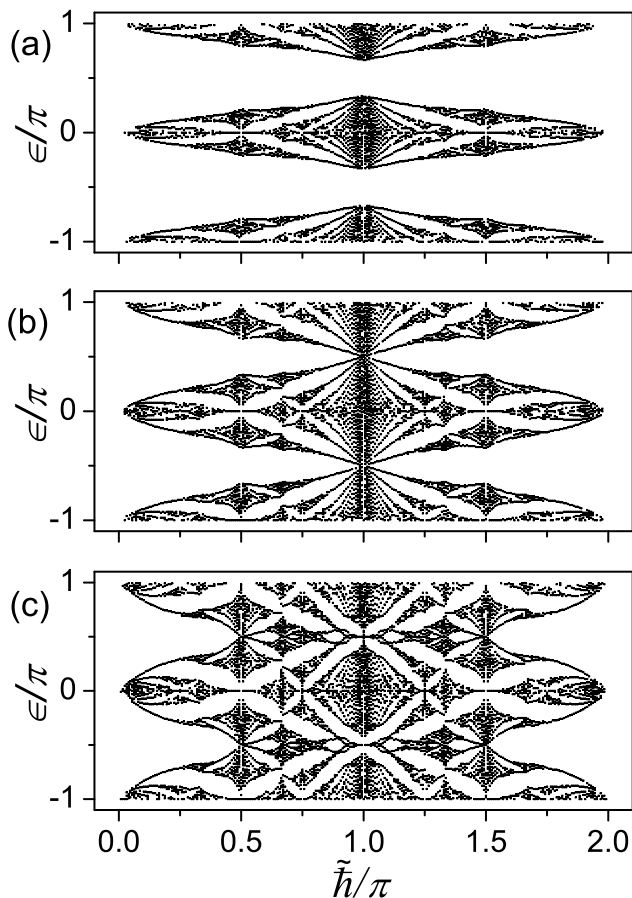


FIG. 3: Quasi-energy spectrum of a double kicked rotor system under the quantum anti-resonance condition $T\hbar = 2\pi$. In panels (a), (b) and (c), $\tilde{K}_1/\tilde{\hbar} = \tilde{K}_2/\tilde{\hbar} = 1.2, \pi/2$, and 2.0 , respectively. In (b), three main branches of the spectrum pattern begin to touch each other. The complex spectrum pattern as a function of $\tilde{\hbar}$ is called “generalized Hofstadter’s butterfly” in the text.

It now becomes interesting to ask whether Hofstadter’s butterfly spectrum also exists for a double kicked rotor system under higher order quantum resonances, i.e., under the condition $T\hbar = 4\pi\nu/\mu$, with ν and μ being integers and with $\mu > 1$. Our preliminary study suggests that this is the case, thus opening up studies of quantum diffusion dynamics in a wider class of quantum mapping systems.

As an example, we present in Fig. 3 the spectrum of the DKRM at the so-called quantum anti-resonance, with $\nu = 1$, $\mu = 2$. For $\tilde{K}_1/\tilde{\hbar} = \tilde{K}_2/\tilde{\hbar} = 0$, the quantum map operator U_{DKRM} in Eq. (6) reduces to $U = e^{-i\pi p^2/\hbar^2}$, yielding only two nonequivalent values of the quasi-energy, i.e., 0 and $\pm\pi$. As $\tilde{K}_1/\tilde{\hbar} = \tilde{K}_2/\tilde{\hbar}$ increases, the complex structure of

the spectrum “grows” around the points 0 and $\pm\pi$. Due to this growth, the spectrum for the case of $K_1/\hbar = \tilde{K}_2/\hbar = 1.2$ is already quite complicated, as seen in Fig. 3(a). When $\tilde{K}_1/\hbar = \tilde{K}_2/\hbar$ reaches $\pi/2$ [see Fig. 3(b)], three main branches of the spectrum begin to touch one another, yielding an overall pattern that can be regarded as a generalized Hofstadter’s butterfly spectrum. With the values of $\tilde{K}_1/\hbar = \tilde{K}_2/\hbar$ increased even further, the generalized Hofstadter’s “butterfly” pattern gets larger and possesses more fine structures. Unaware of any study with similar results, we think that the generalized “butterfly” spectrum found here and those associated with other higher-order quantum resonances will stimulate considerable theoretical work. The results further strengthen the view that using controlled laser-matter interactions, novel quantum dynamics models may be generated and explored.

IV. CONCLUSION

To conclude, we have shown that by considering a cold-atom realization of an on-resonance double kicked rotor model we can realize a quantum version of the kicked Harper model from a kicked rotor system. To the naked eye, the butterfly spectrum we obtain from our version of a kicked Harper model is almost indistinguishable from that of the standard kicked Harper model. We have also stressed that the effective Planck constant of the quantum kicked Harper model realized here can be easily tuned by varying the time delay between two sequences of control fields. Extending our considerations to double kicked rotor systems under higher-order quantum resonances, we have shown that an entirely new class of quantum mapping systems with generalized Hofstadter’s butterfly spectra can be studied, both theoretically and experimentally. These results present many new opportunities in the studies of quantum nonlinear dynamics in external control fields. Indeed, with controlled interactions between laser fields and cold atoms, there are still so much to see and explore.

V. ACKNOWLEDGMENTS

Two of the authors (J.W. and J.G.) are very grateful to Prof. C.-H. Lai for his support and encouragement. One of the authors (J.W.) acknowledges support from Defence Science and Technology Agency (DSTA) of Singapore under agreement of POD0613356. One of the authors (A.S.M.) is supported by a Villum Kann Rasmussen grant. One of the authors

(J.G.) is supported by the start-up fund (WBS No. R-144-050-193-101/133), and the NUS “YIA” fund (WBS No. R-144-000-195-123) from the office of Deputy President (Research & Technology), National University of Singapore.

- [1] M. Shapiro and P. Brumer, *Principles of the Quantum Control of Molecular Processes* (Wiley, New York, **2003**).
- [2] S.A. Rice and M. Zhao, *Optical Control of Molecular Dynamics* (Wiley, New York, **2000**).
- [3] J.B. Gong and P. Brumer, *Ann. Rev. Phys. Chem.* **2005**, 56, 1-23; *Phys. Rev. Lett.* **2001**, 86, 1741-1744; *Phys. Rev. E* **2004**, 70, 016202; *Phys. Rev. E* **2003**, 68, 056202.
- [4] G. Casati, B.V. Chirikov, F.M. Izraelev, J. Ford, *Lecture Notes in Physics* Vol. 93 (Springer, Berlin, **1979**), pp. 334.
- [5] F.M. Izrailev, *Phys. Rep.* **1990**, 196, 299-392.
- [6] S. Fishman, D.R. Grempel, R.E. Prange, *Phys. Rev. Lett.* **1982**, 49, 509-512.
- [7] F.L. Moore, J.C. Robinson, C.F. Bharucha, B. Sundaram, M.G. Raizen, *Phys. Rev. Lett.* **1995**, 75, 4598-4601.
- [8] H. Ammann, R. Gray, I. Shvarchuck, N. Christensen, *Phys. Rev. Lett.* **1998**, 80, 4111-4114; M.K. Oberthaler, R.M. Godun, M.B. d’Arcy, G.S. Summy, K. Burnett, *Phys. Rev. Lett.* **1999**, 83, 4447-4451; P. Szriftgiser, J. Ringot, D. Delande, J.C. Garreau, *Phys. Rev. Lett.* **2002**, 89, 224101; G. Duffy, S. Parkins, T. Muller, M. Sadgrove, R. Leonhardt, and A.C. Wilson, *Phys. Rev. E* **2004**, 70, 056206; P.H. Jones, M. Goonasekera, D.R. Meacher, T. Jonckheere, T.S. Monteiro, *Phys. Rev. Lett.* **2007**, 98, 073002.
- [9] M. Sadgrove, M. Horikoshi, T. Sekimura, and K. Nakagawa, *Phys. Rev. Lett.* **2007**, 99, 043002.
- [10] I. Dana, V. Ramareddy, I. Talukdar, and G.S. Summy, *Phys. Rev. Lett.* **2008**, 100, 024103.
- [11] T. Geisel, R. Ketzmerick, and G. Petschel, *Phys. Rev. Lett.* **1991**, 67, 3635-3638.
- [12] R. Lima, and D. Shepelyansky, *Phys. Rev. Lett.* **1991**, 67, 1377-1380.
- [13] R. Artuso, F. Borgonovi, I. Guarneri, L. Rebuzzini, and G. Casati, *Phys. Rev. Lett.* **1992**, 69, 3302-3304.
- [14] T. Prosen, I.I. Satija, and N. Shah, *Phys. Rev. Lett.* **2001**, 87, 066601.
- [15] J.B. Gong and P. Brumer, *Phys. Rev. Lett.* **2006**, 97, 240602.
- [16] D.R. Hofstadter, *Phys. Rev. B* **1976**, 14, 2239-2249.

- [17] J.Wang and J.B. Gong, *Phys. Rev. A* **2008**, (Rapid Communication), in press. See also arXiv: 0711.3939.
- [18] P.H. Jones, M.M.A. Stocklin, G. Hur, T.S. Monteiro, *Phys. Rev. Lett.* **2004**, 93, 223002; C.E. Creffield, G. Hur, T.S. Monteiro, *Phys. Rev. Lett.* **2006**, 96, 024103; C.E. Creffield, S. Fishman, T.S. Monteiro, *Phys. Rev. E* **2006**, 73, 066202.
- [19] J. Wang, T.S. Monteiro, S. Fishman, J.P. Keating, and R. Shubert, *Phys. Rev. Lett.* **2007**, 99, 234101.
- [20] A. Matzkin, and T.S. Monteiro, *Phys. Rev. E* **2004**, 70, 046215.
- [21] J.B. Gong and J. Wang, *Phys. Rev. E* **2007**, 76, 036217.
- [22] R. Artuso, G. Casati, and D. Shepelyansky, *Phys. Rev. Lett.* **1992**, 68, 3826-3829.
- [23] A. Iomin and S. Fishman, *Phys. Rev. Lett.* **1998**, 81, 1921-1924.
- [24] I. Dana, *Phys. Lett. A* **1995**, 197, 413-416.
- [25] I. Dana, *Phys. Rev. Lett.* **1994**, 73, 1609-1612.
- [26] T. Geisel, R. Ketzmerick, and G. Petschel, *Phys. Rev. Lett.* **1991**, 66, 1651-1654.
- [27] J. Wang, A. Mouritzen, and J.B. Gong (in preparation).